Supporting Information for

Genesis of Bi-functional Acid-Base Site on Cr-supported Layered Double Hydroxide Catalyst Surface for One-pot Synthesis of Furfurals from Xylose with Solid Acid Catalyst

Mahiro Shirotori,[a] *Shun Nishimura*,[a,b] and *Kohki Ebitani* [a,b]
[a]School of Materials Science, Japan Advanced Institute of Science and Technology,
1-1Asahidai, Nomi, Ishikawa 923-1292, Japan
[b]Graduate School of Advanced Science and Technology, Japan Advanced Institute of Science and Technology

Contents

Synthesis of Cr/Supports

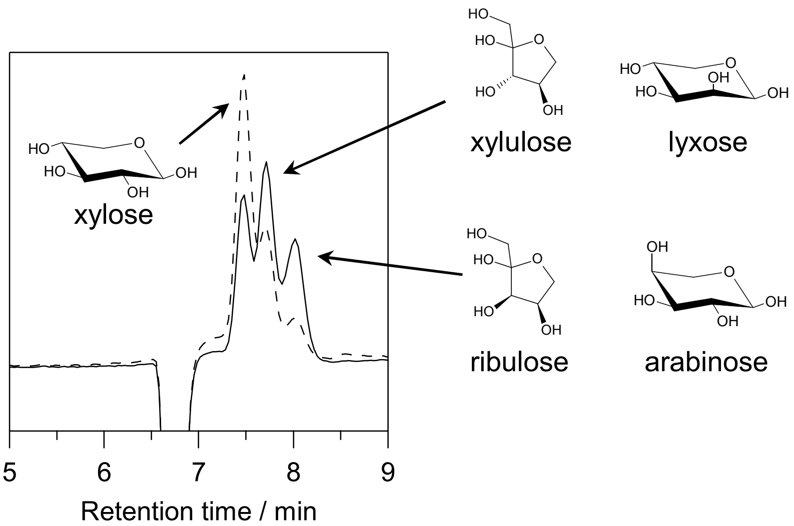

Figure S1. HPLC chart of transformation of xylose using Mg-Al LDH (dashed line) and 9wt%Cr/Mg-Al LDH (solid line). *Reaction conditions:* xylose (0.67 mmol), catalyst (0.2 g), *N*,*N*-dimethylformamide (3 mL), 373 K, 3 h, 500 rpm, and N_2 flow (30 mL min^{-1}).

Table S1. Rough calculated conversion and selectivity values for isomerization of xylose over Mg-Al LDH and 9wt%Cr/Mg-Al LDH.

Catalyst	Conversion of xylose /%	Selectivity for isomerized pentoses /%
9wt%Cr/Mg-Al LDH	~80	~55
Mg-Al LDH	~60	~30

Reaction conditions: xylose (0.67 mmol), catalyst (0.2 g), *N*,*N*-dimethylformamide (3 mL), 373 K, 3 h, 500 rpm, N_2 flow (30 mL min^{-1}). The three HPLC peaks attributed to (A) xylose, (B) xylulose and lyxose, and (C) ribulose and arabinose were divided by curve fitting with a Gaussian function. The saccharide amounts of each peak were calculated using the absolute calibration method with a coefficient based on xylose for peak (A), the average of xylulose and lyxose for peak (B), and the average of ribulose and arabinose for peak (C).

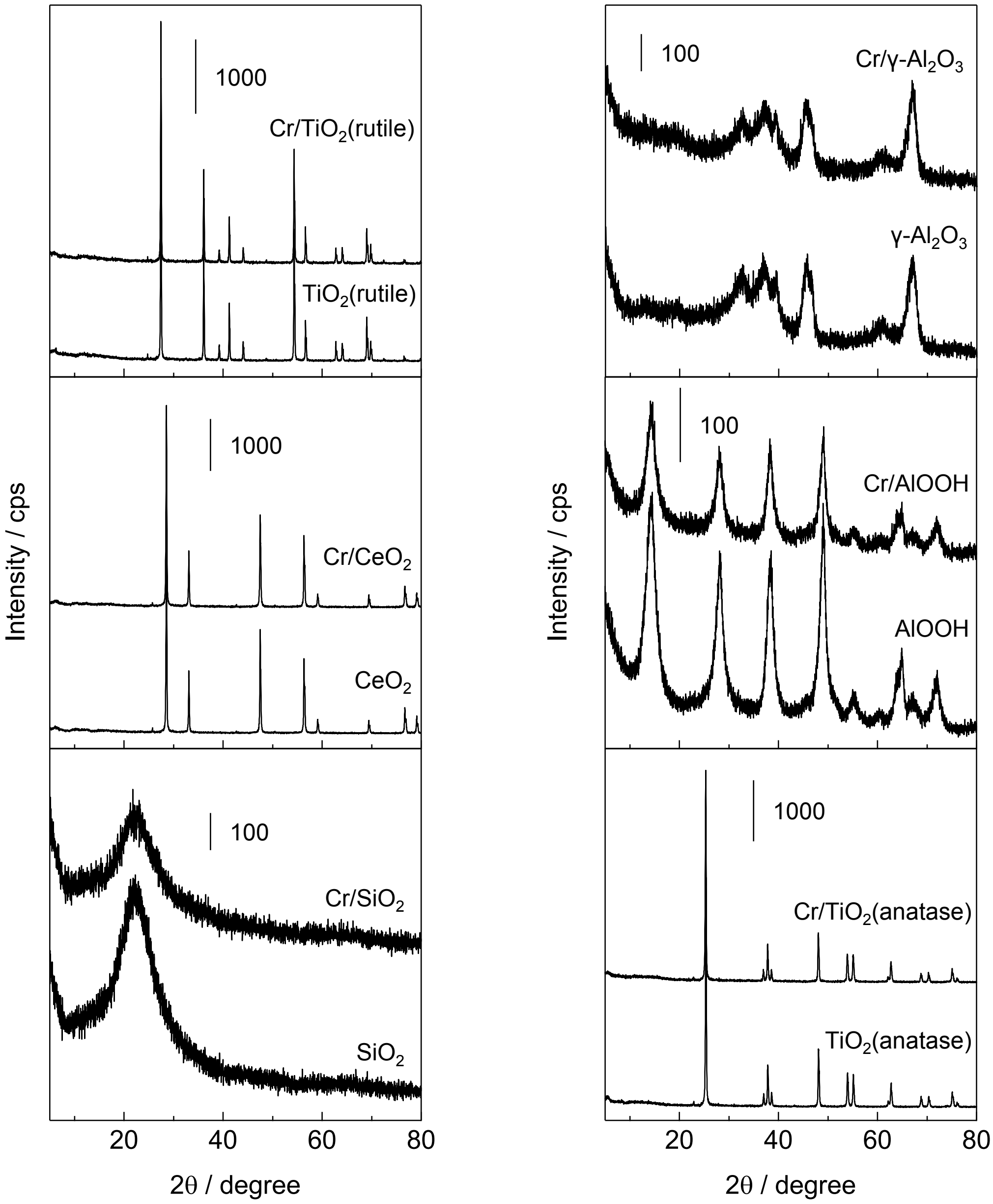

Figure S2. XRD patterns of various supports and Cr supported catalysts with 9 wt% Cr loading.

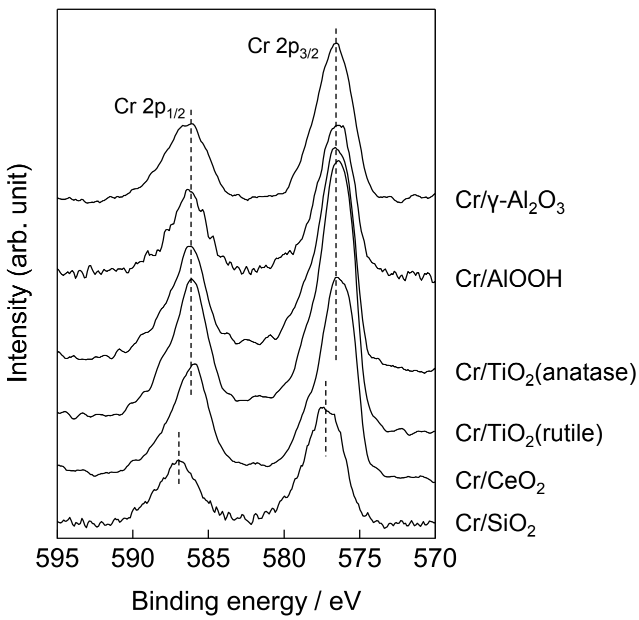

Figure S3. Cr 2p XPS of various Cr supported catalysts with 9 wt% Cr loading.

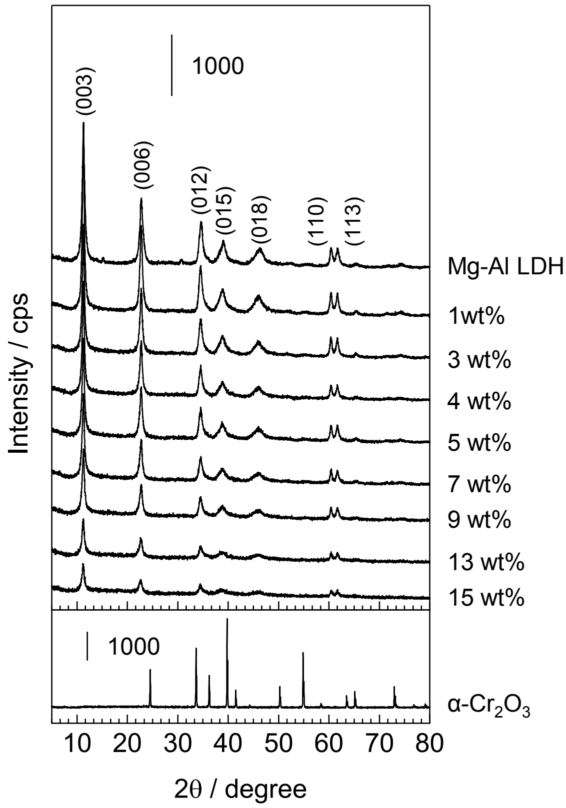

Figure S4. XRD patterns of Cr/Mg-Al LDHs with various Cr loadings.

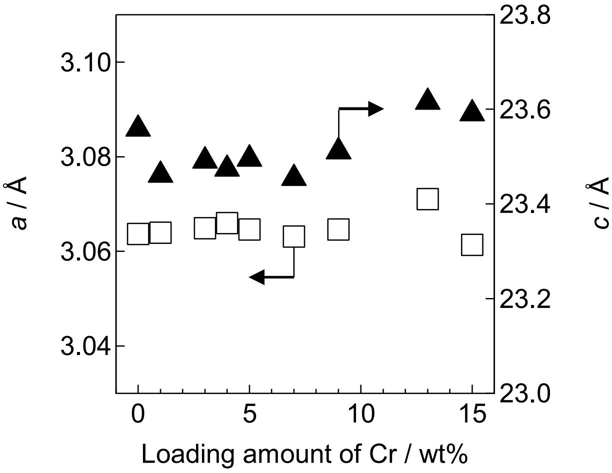

Figure S5. Lattice parameter *a* and *c* of Cr/Mg-Al LDHs with various Cr loadings.

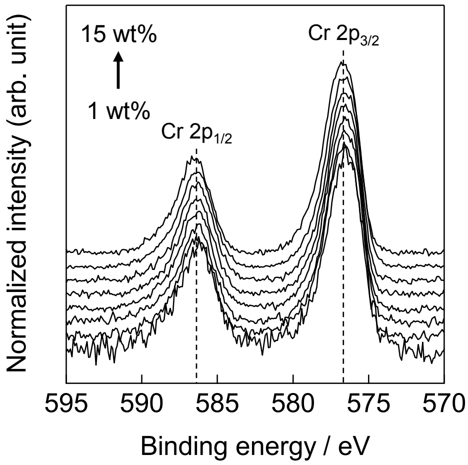

Figure S6. Normalized Cr 2p XPS of Cr/Mg-Al LDHs with various Cr loadings.

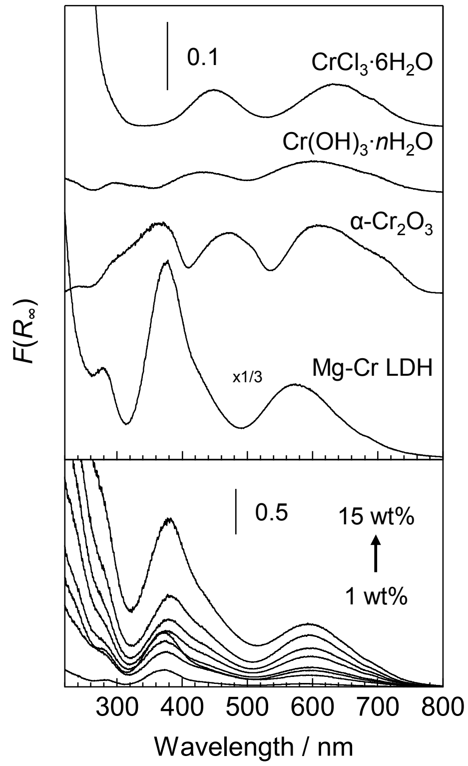

Figure S7. DR UV-vis spectra of Cr/Mg-Al LDH with various Cr loadings and α-Cr_2O_3, $Cr(OH)_3 \cdot nH_2O$, $CrCl_3 \cdot 6H_2O$ and Mg-Cr LDH as reference samples. α-Cr_2O_3, $Cr(OH)_3 \cdot nH_2O$, and $CrCl_3 \cdot 6H_2O$ are diluted 10 times with $BaSO_4$. DR UV-vis spectra were collected on a U-3900H (Hitachi) at wavelengths of 220–800 nm with a scan rate of 120 nm min^{-1}.

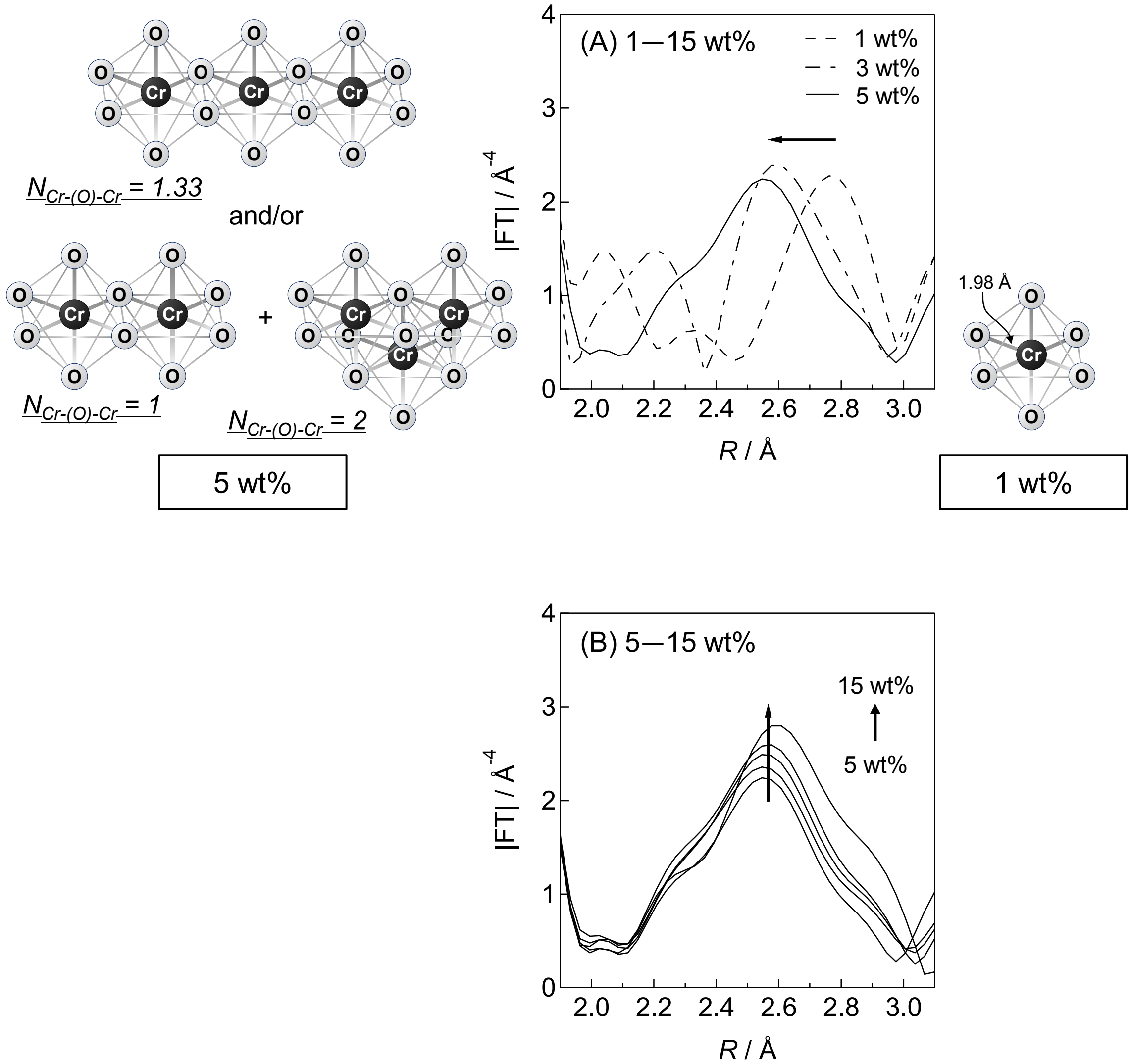

Figure S8. Fourier transforms of Cr *K*-edge k^3-weighted EXAFS of Cr/Mg-Al LDHs with various Cr loadings. (A) 1–5 wt% and (b) 5–15 wt%Cr/Mg-Al LDHs.

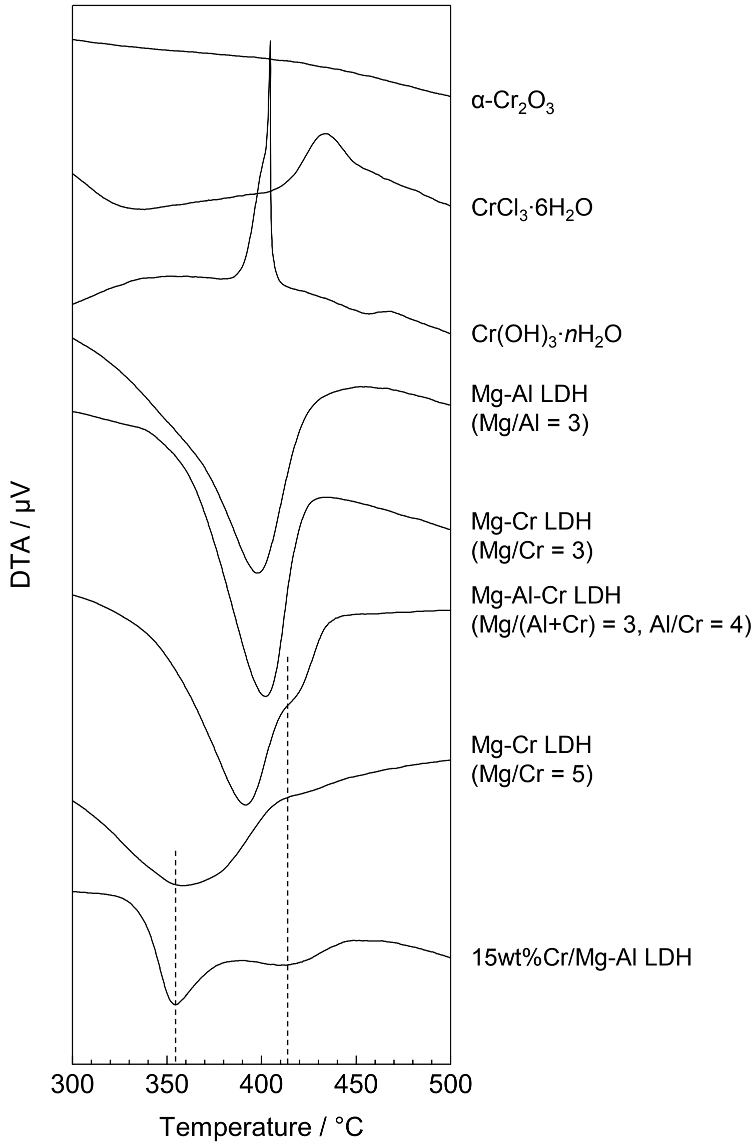

Figure S9. DTA of 15wt%Cr/Mg-Al LDH and Cr^{3+} references.

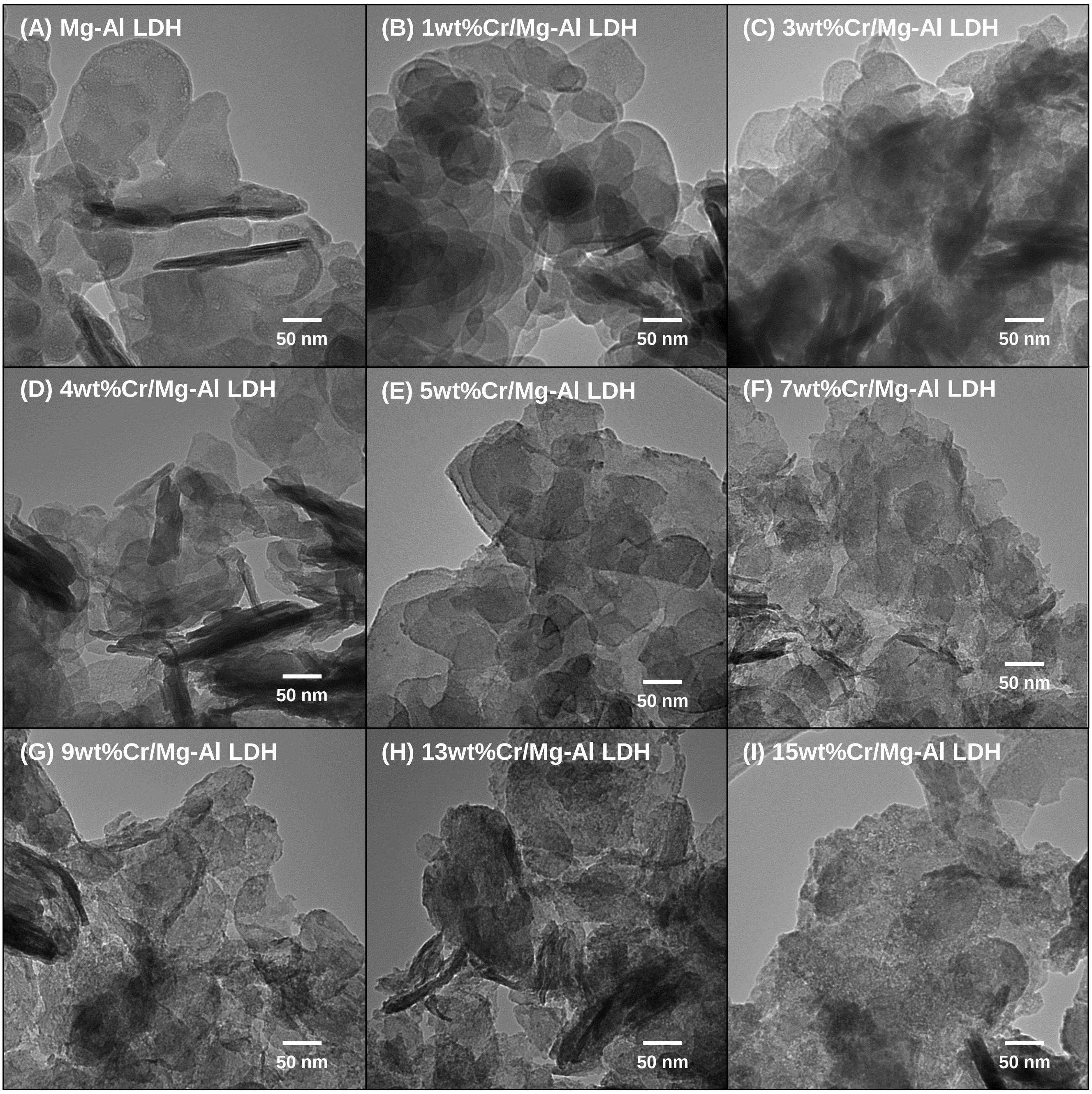

Figure S10. TEM images of Mg-Al LDH and Cr/Mg-Al LDHs with various Cr loadings: (A) Mg-Al LDH, (B) 1wt%-, (C) 3wt%-, (D) 4wt%-, (E) 5wt%-, (F) 7wt%- (G) 9wt%-, (H) 13wt%-, and (I) 15wt%Cr/Mg-Al LDH.

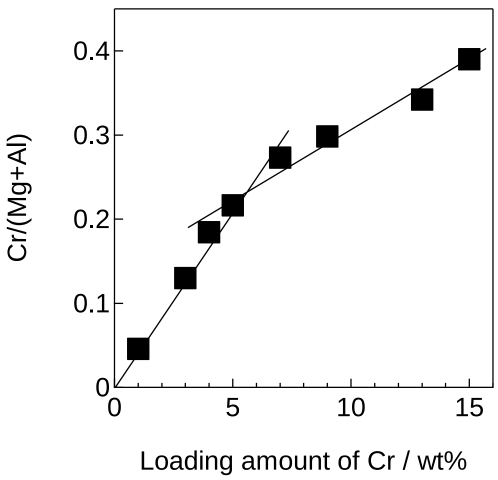

Figure S11. Atomic ratio of Cr/Mg-Al LDHs with various Cr loadings. Atomic ratios were calculated based on Cr 2p, Mg 2p, and Al 2p XPS.

Table S2. Physical properties of Cr/Mg-Al LDHs with various Cr loadings

Cr content				S_{BET}[c] / m^2 g^{-1}	S_0[d] / m^2	$S_{occupied}$[e] / m^2 g(cat)$^{-1}$	$S_{occupied}$[e] / m^2 g(Mg-Al LDH)$^{-1}$	θ[f] /%
mmol g(Mg-Al LDH)$^{-1}$	wt% as Cr[a]	wt% as Cr[b]	wt% as Cr_2O_3[a]					
0	0	0	0	44.5	44.5	0	0	0
0.19	1	1.0	1.5	55.8	56.6	18.1	18.3	32.3
0.60	3	3.1	4.3	71.8	75.0	54.5	56.2	74.8
0.80	4	4.0	5.7	73.6	78.1	72.6	75.6	96.8
1.02	5	5.1	7.2	83.6	90.1	91.6	96.4	107
1.45	7	7.7	9.9	96.3	107	127	137	128
1.90	9	9.7	12.6	140	160	163	180	112
2.87	13	14.6	17.9	190	232	236	271	117
3.39	15	15.9	20.5	238	299	272	320	107

[a]Theoretical value. [b]Obtained by ICP-AES. [c]BET specific surface area. [d]Surface area of g(Mg-Al LDH)$^{-1}$ carrier. [e]Occupied area by Cr_2O_3 unit (0.16 nm^2). [f]Coverage of Cr_2O_3 on Mg-Al LDH.
Cross section of Cr_2O_3 unit on Mg-Al LDH was calculated as the cluster composed of two edge-sharing CrO_6 octahedral using the length of Cr-O (0.198 nm) obtained from EXAFS curve fitting.

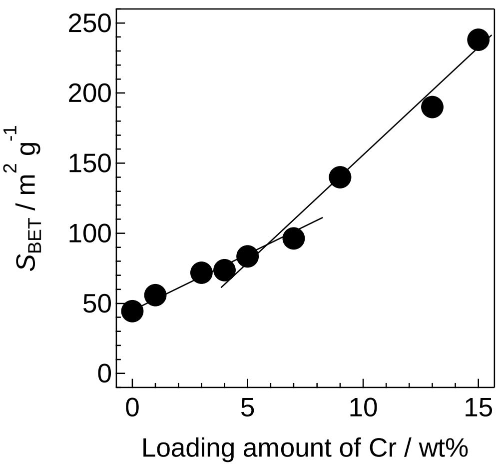

Figure S12. Specific surface area of Cr/Mg-Al LDHs with various Cr loadings.

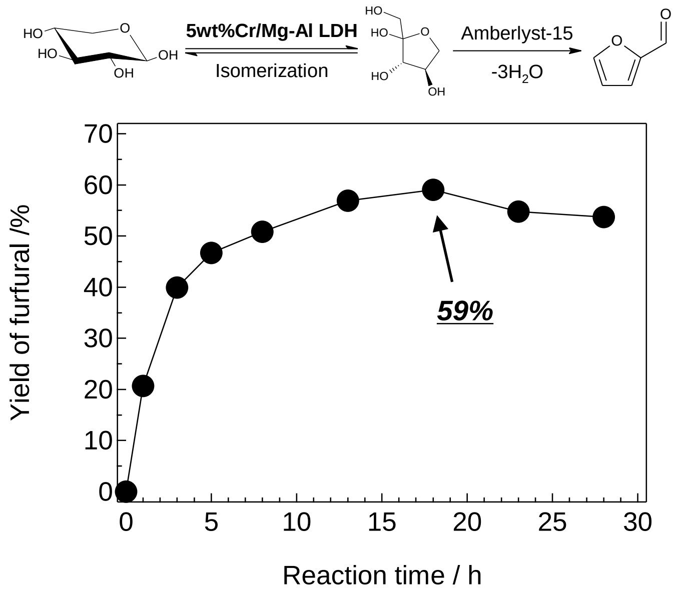

Figure S13. Time cause of furfural yield in the one-pot transformation of xylose using 5wt%Cr/Mg-Al LDH and Amberlyst-15. *Reaction conditions:* xylose (0.67 mmol), 5wt%Cr/Mg-Al LDH (0.2 g), Amberlyst-15 (0.1 g), *N*,*N*-dimethylformamide (3 mL), 373 K, 500 rpm, and N_2 flow (30 mL min^{-1}).

Synthesis of Cr/Supports

Cr-supported SiO_2, CeO_2, TiO_2(rutile), TiO_2(anatase), AlOOH, and γ-Al_2O_3 (Cr: 9 wt%) were prepared by an impregnation method (adsorption) using various supports and an aqueous solution of $CrCl_3{\cdot}6H_2O$ and urea: $CrCl_3{\cdot}6H_2O$ was dissolved in 50 mL of distilled water; then 1 g of support and 2 g of urea were added. After stirring at 353 K for 24 h, the obtained paste was filtered, washed with 2 L of distilled water, and then dried at 383 K overnight.